

Multiple Pion Production in Interactions of Positive Pions with Protons Near 1 BeV*

HORST W. J. FOELSCH† AND HENRY L. KRAYBILL

Yale University, New Haven, Connecticut

(Received 29 August 1963; revised manuscript received 27 December 1963)

We report results of a study of multiple pion production in the reactions $\pi^+p \rightarrow p\pi^+\pi^+\pi^-$ and $\pi^+p \rightarrow p\pi^+\pi^+\pi^-\pi^0$ at pion kinetic energies 910 MeV, 1090 MeV, and 1260 MeV. Double pion production is dominated by production of the $N^*(\frac{3}{2}, \frac{3}{2})$ nucleon isobar and no other resonant states among the outgoing particles are identified. Triple pion production proceeds almost entirely by formation of the η meson (mass 549 MeV) which subsequently decays into $(\pi^+\pi^-\pi^0)$. The isotopic spin of the η is confirmed to be $I=0$ and the spin J , parity P , and G -parity G are confirmed to be most likely $J^{PG}=0^{-+}$. The relative decay rate $(\eta \rightarrow \pi^+\pi^-\gamma)/(\eta \rightarrow \pi^+\pi^-\pi^0)$ is found to be 0.14 ± 0.08 , and the decay ratio $(\eta \rightarrow 3\pi^0)/(\eta \rightarrow \pi^+\pi^-\pi^0)$ is found to be 2 ± 1 . No η 's were observed at 910 MeV. At 1090 MeV and 1260 MeV, the production angular distributions of the η are roughly isotropic. η production appears to be associated with the production of the $N^*(\frac{3}{2}, \frac{3}{2})$ isobar, in the (p, π^+) system.

I. INTRODUCTION

THE production of several pions in elementary particle interactions has become of paramount interest since it was discovered that very often the process occurs by production of resonant states which subsequently decay into the particles observed. The production of these states is relevant to theories of the structure of the target nucleons.¹

In the spring of 1961 a strong resonant state in the $(\pi\pi)$ system, the ρ meson of mass 750 MeV and ≈ 100 MeV width, was discovered² in interactions of π mesons in hydrogen bubble chambers, by observing the spectrum of the "effective mass" (invariant mass) of two pions in the final state. For N particles this effective mass M is given by the Lorentz-invariant expression

$$M^2 = (\sum_i^N E_i)^2 - (\sum_i^N P_i)^2,$$

where E_i and P_i are the energy and momentum of each particle, and units are such that $c=1$. The ρ meson has since been observed in various experiments and its quantum numbers have been established as: isotopic spin $I=1$, angular momentum J , parity P , and G parity G , $J^{PG}=1^{-+}$.

After the discovery of the ρ meson a second particle, the ω meson, was discovered³ in antiproton-proton annihilations to decay into three pions (π^+ , π^- , π^0). The discoverers established the quantum numbers of the ω to be $I=0$, $J^{PG}=1^{-}$.

* This research was partially supported by the U. S. Atomic Energy Commission.

† Part of this work was submitted by H. Foelsche in partial fulfillment of the requirements for the degree of Doctor of Philosophy at Yale University, 1963.

¹ W. Frazer and J. Fulco, Phys. Rev. Letters **2**, 365 (1959); Y. Fujii, Progr. Theoret. Phys. (Kyoto) **21**, 232 (1959); G. Breit, Proc. Nat. Acad. Sci. U. S. **46**, 746 (1960); Phys. Rev. **120**, 287 (1960).

² A. Erwin, R. March, W. Walker and E. West, Phys. Rev. Letters **6**, 628 (1961); D. Stonehill, C. Baltay, H. Courant, W. Fickinger, E. C. Fowler *et al.*, *ibid.* **6**, 624 (1961); E. Pickup, D. K. Robinson, and E. O. Salant, *ibid.* **7**, 192 (1961); J. Anderson, V. Bang, P. Burke, D. Carmony, and N. Schmitz, *ibid.* **6**, 365 (1961).

³ M. L. Stevenson, L. W. Alvarez, B. C. Maglic, and A. H. Rosenfeld, Phys. Rev. Letters **7**, 178 (1961); Phys. Rev. **125**, 687 (1962).

Particles with the quantum numbers above had been predicted in theoretical interpretations of the observed electromagnetic structure of the nucleon.

Shortly after the discovery of the ω meson its existence was confirmed by Pevsner *et al.*⁴ in reactions of positive π mesons in deuterium. In addition, this group discovered the η meson of mass ≈ 546 MeV, in the same effective mass spectrum. The existence of the η was confirmed with small but conclusive statistics by Bastien *et al.*⁵ They suggested that its quantum numbers are $J^{PG}=0^{-+}$, starting from an argument by Carmony *et al.*⁶ showing that the isotopic spin is $I=0$.

The experiment reported in this paper was undertaken in order to study the multiple pion production mechanism in interactions of positive π mesons with protons, in reactions of the type

- (1) $\pi^+p \rightarrow \pi^+p\pi^+\pi^-$,
- (2) $\pi^+p \rightarrow \pi^+p\pi^+\pi^-\pi^0$,

at incident-pion kinetic energies of 910, 1090, and 1260 MeV.

It was expected that the resonance at 1238 MeV in the $(p\pi^+)$ system would be prominent, and it was hoped that the production mechanism for the remaining pions would become apparent. Sufficient energy is present at 1090 MeV and at 1260 MeV to create the η meson and also the so-called ζ meson of mass $M \approx 580$ MeV which had been claimed to be observed⁷ in the effective mass spectrum of two π mesons. The available energy, however, is insufficient to produce either the ρ meson or the ω meson.

⁴ A. Pevsner, R. Kraemer, J. Nussbaum, C. Richardson, P. Schlein *et al.*, Phys. Rev. Letters **7**, 421 (1961).

⁵ P. L. Bastien, J. P. Berge, O. I. Dahl, M. Ferro-Luzzi, D. H. Miller *et al.*, Phys. Rev. Letters **8**, 114 (1962).

⁶ D. D. Carmony, A. H. Rosenfeld, and R. T. Van de Walle, Phys. Rev. Letters **8**, 117 (1962).

⁷ R. Barloutaud, J. Heughebaert, A. Leveque, J. Meyer, and R. Ommes, Phys. Rev. Letters **8**, 32 (1962); C. Peck, L. Jones, M. Perl, Technical Report No. 4, University of Michigan, 1962 (unpublished); B. Sechi Zorn, Phys. Letters **8**, 282 (1962).

The preliminary results^{8,9} of this investigation have determined its later course. It was found that the η meson was formed in nearly all cases of reaction (2). This provided the opportunity to study the quantum numbers of the η using a sizeable sample with very little background. It was also possible to search for other decay modes of the η , namely the (π^+, π^-, γ) decay, and—by observation of the decay of $\pi^0 \rightarrow (e^+, e^-, \gamma)$ —the $(3\pi^0)$ decay. The production states of the η meson have also been studied.

The following section represents a brief summary of the analytical methods which are used to discuss the experimental results. In the next section we describe the experimental conditions and the data reduction process. The results on the production of two pions [reaction (1)], and the investigations of the η meson are presented in the last three sections.

II. THEORETICAL REMARKS

(a) Production Dalitz Plot

In discussing a final state of three particles it is useful to exhibit the kinematic correlations of the particles in a Dalitz plot.¹⁰ The kinetic energies of two of the outgoing particles, measured in the three-particle center of mass, are plotted as Cartesian coordinates. It is a convenient property of this plot that a unit of area in the allowed region is proportional to a unit of Lorentz-invariant phase space.¹¹ Thus, if the Lorentz-invariant phase space is uniformly populated, the corresponding Dalitz plot will show a constant density of points.¹⁰

Let E_i , P_i be the total energy and momentum of particle i , in the reaction center of momentum. For constant E_1 there is a strip of allowed values of E_2 , for the three-body final state. Along this strip the “effective mass” of particles two and three is constant, namely,

$$\begin{aligned} M_{23}^2 &= (E_2 + E_3)^2 - (P_2 + P_3)^2 \\ &= (E_1^2 + M_1^2) - 2E_1E_2, \end{aligned}$$

where E_i is the total energy in the center of momentum of the reaction, and M_1 is the mass of particle one.

Considering M_{23} as a particle which decays into particles two and three, and defining θ as the “decay” angle measured in the M_{23} rest frame between particle 2 and the line of flight M_{23} , one can show that the $\cos\theta$ is a linear function of E_2 for constant E_1 . Thus, if a resonant state or particle of mass M_{23} is produced, the

Dalitz plot will show a concentration of events along a strip of constant E_1 and the density of points will vary along the strip as the angular distribution $dN/d\cos\theta$.

(b) Decay Dalitz Plot

A variation of the above approach was introduced by Dalitz¹⁰ long ago in discussions of the three-pion decay of the τ meson. The data on the decay of a particle into three particles of equal mass (e.g., $\pi^+\pi^-\pi^0$) are represented in a triangular plot. Since in an equilateral triangle the sum of the distances of an interior point from the sides is constant, one may let the distances from the three sides represent the kinetic energies T_i of the three particles. Energy conservation is satisfied if a point lies inside the limiting triangle. Momentum conservation restricts the points to be inside an inscribed circle if the three particles are nonrelativistic, an inscribed equilateral triangle in the extreme relativistic case, or some intermediate figure in general.

Figure 8 represents such a plot for the η meson which has a mass of 549 MeV ($Q=135$ MeV). The boundary of this plot corresponds to the collinear decay configuration of the three particles and the medians of the triangle are the locus of points where two kinetic energies are equal.

The triangular Dalitz plot has the property that a unit of area represents a unit of Lorentz-invariant phase space. The plot also conveniently exhibits the symmetry properties of matrix elements with respect to permutation of the particles. These symmetry properties can be derived from the quantum numbers of the parent particles and the final state of three pions. In making such predictions it is customary to assume that the simplest possible matrix element is predominant since more complex elements will involve high angular momentum states with stronger barrier factors. These matrix elements have been frequently discussed in previous publications, and an extensive table has recently been published.¹²

Table I exhibits matrix elements for the quantum numbers $I=0$ or 1 , $J=0$ or 1 , $P=\pm 1$, and $G=\pm 1$, in all possible combinations. Table I also indicates whether or not the transition conserves isotopic spin, and on which parts of the Dalitz plot the matrix element is required to vanish. Isospin-violating matrix elements are listed only if the decay by strong interactions is forbidden.

The predictions of the simplest matrix elements need not always conform to the actual physical situation. Generally they indicate only at what points on the Dalitz plot the transition amplitudes must vanish. Special dynamical properties of the system, such as preferred emission of two pions with a certain isospin and unique effective mass, would introduce additional variation of the matrix element with the energies of the decay pions. The possibility of such a deviation will be

⁸ H. Foelsche, E. C. Fowler, H. L. Kraybill, J. R. Sanford, and D. Stonehill, in *Proceedings of the 1962 International Conference on High Energy Physics at CERN*, edited by J. Prentki (CERN, Geneva), p. 36.

⁹ H. Foelsche, E. C. Fowler, H. L. Kraybill, J. R. Sanford, and D. Stonehill, *Phys. Rev. Letters* **9**, 223 (1962).

¹⁰ R. H. Dalitz, *Phil. Mag.* **44**, 1068 (1953); *Phys. Rev.* **91**, 1046 (1954); E. Fabri, *Nuovo Cimento* **11**, 479 (1954); M. Gell-Mann and A. Rosenfeld, *Ann. Rev. Nucl. Sci.* **7**, 407 (1957).

¹¹ For the meaning of Lorentz invariant phase space, see for example P. P. Srivastava and G. Sudarshan, *Phys. Rev.* **110**, 765 (1958).

¹² E. M. Henley and B. A. Jacobsohn, *Phys. Rev.* **128**, 1394 (1962).

TABLE I. Three-pion decay matrix elements.

Quantum Numbers of the Meson				Matrix element ^a	On Dalitz plot, matrix element vanishes at
$I=0$		$I=1$			
J^{PG}	Isospin conserved?	J^{PG}	Isospin conserved?		
0^{-}	Yes	0^{-+}	No	$E_1^2(E_2-E_3)+E_2^2(E_3-E_1)+E_3^2(E_1-E_2)$ (E_1-E_2)	3 axes Y axis
1^{+-}	Yes	1^{++}	No	$\mathbf{p}_1(E_2-E_3)+\mathbf{p}_2(E_3-E_1)+\mathbf{p}_3(E_1-E_2)$	center, maximum energies
1^{-}	Yes	1^{-+}	No	$\mathbf{p}_1-\mathbf{p}_2$	maximum energy of π^0
0^{-+}	No	0^{-}	Yes	$\mathbf{p}_1\times\mathbf{p}_2+\mathbf{p}_2\times\mathbf{p}_3+\mathbf{p}_3\times\mathbf{p}_1=3\mathbf{p}_1\times\mathbf{p}_2$	boundary
1^{++}	No	1^{+-}	Yes	constant	nowhere
1^{-+}	No	1^{-}	Yes	$\mathbf{p}_1+\mathbf{p}_2-2\mathbf{p}_3$	$Y=0$ only
		1^{-}	Yes	$(E_1-E_2)(\mathbf{p}_1\times\mathbf{p}_2+\mathbf{p}_2\times\mathbf{p}_3+\mathbf{p}_3\times\mathbf{p}_1)$	Y axis, boundary

^a E_i = Energies of particles; $1 = \pi^+$, $2 = \pi^-$, $3 = \pi^0$. \mathbf{p}_i = Momenta of particles 1, 2, 3. All quantities measured in the rest frame of parent boson.

discussed in Sec. V in connection with the decay Dalitz plot of the η meson.

III. THE EXPERIMENT

The 20-in. hydrogen bubble chamber¹³ of Brookhaven National Laboratory was exposed to a beam of positive π mesons at incident pion kinetic energies of 910, 1090, and 1260 MeV. Nine thousand frames were taken at 910, 85 000 at 1090 MeV, and 8000 at 1260 MeV, using an electrostatically separated π^+ beam at the Cosmotron (see Baltay, Sandweiss *et al.*, Ref. 14). An additional 20 000 pictures at 1260 MeV were obtained later with the separated beam at the A. G. S. (see Baltay, Sandweiss *et al.*, Ref. 14) in Brookhaven using the same chamber. The entire exposure was scanned for interactions with four outgoing charged tracks, and the scanners found 100, 1700, and 1200 events at the energies 910, 1090, and 1260 MeV, respectively. Events were measured on the digitized "Franckenstein" reprojectors or on a manually operated measuring machine (MOLE) designed and constructed at Yale. The computer program YACK, which incorporates spatial reconstruction routines and the kinematic fitting routine GUTS, subjected the measurements to fits of the types

- (1) $\pi^+p \rightarrow \pi^+p\pi^+\pi^-$,
- (2) $\pi^+p \rightarrow \pi^+p\pi^+\pi^-\pi^0$,
- (3) $\pi^+p \rightarrow \pi^+\pi^+\pi^+\pi^-\pi^0$

by minimizing the quantity

$$\chi^2 = \sum_{ij} (x_i - x_i^m) G_{ij} (x_j - x_j^m)$$

¹³ D. Rahm, Proceeding International Conference of High Energy Accelerators and Instrumentation of High Energy Physics, Berkeley, 1960 (unpublished).

¹⁴ J. R. Sanford, Ph.D. dissertation, Yale University (unpublished); C. Baltay, H. Courant, W. J. Fickinger, E. C. Fowler, H. L. Kraybill *et al.*, Rev. Mod. Phys. **33**, 374 (1961); C. Baltay, J. Sandweiss, J. R. Sanford, H. Brown, M. Webster, S. Yamamoto, in *Proceedings of the 1962 Conference on Instrumentation for High Energy Physics at CERN*, edited by F. J. M. Farley and M. E. Meyer (North-Holland Publishing Company, Amsterdam, 1963).

subject to the constraints of energy and momentum conservation. Here x_i^m are measured values of parameters which yield the angles and momenta of tracks at the production vertex, x_i are the readjusted values consistent with the constraints, and G_{ij} are the elements of the Gaussian error correlation matrix. The program was also used to study four-pronged events of the type

- (4) (a) $\pi^+p \rightarrow \pi^+pX^0$,
- (b) $X^0 \rightarrow e^+e^-$ neutrals

with a missing neutral X^0 giving rise to internally converted electron pairs (4b). An event was positively identified if all of the following criteria were satisfied:

(a) Each track measurement was required to be reasonably consistent with a fit to a helix. This test of the quality of the track measurement had to be relaxed for tracks which lose a substantial fraction of their energy along their measurable path.

(b) The upper limit of χ^2 was 30.0 for fits without any missing neutrals (4 constraints) and 9.0 for events with one identified missing neutral (one constraint).

(c) A satisfactory fit had to agree with the bubble density of each track as observed on a reprojector. In this energy region a proton can nearly always be distinguished from a π meson by bubble density.

The minimized values of χ^2 should have average values of 4.0 (four constraints) and 1.0 (one constraint), respectively, if the experimental errors were correctly assessed and Gaussian. The experimental distributions show (Fig. 1) average values of 8.2 and 1.7, respectively, and the theoretical distributions fit well after they are expanded by the ratio of the experimental and theoretical averages. These circumstances indicate that the errors are larger than estimated in our programs, by factors equal to the square root of the required expansion factors.

The data presented in the subsequent sections represent a complete analysis of the available film except that only 95% of all examples of reaction (1) at 1090 MeV are shown.

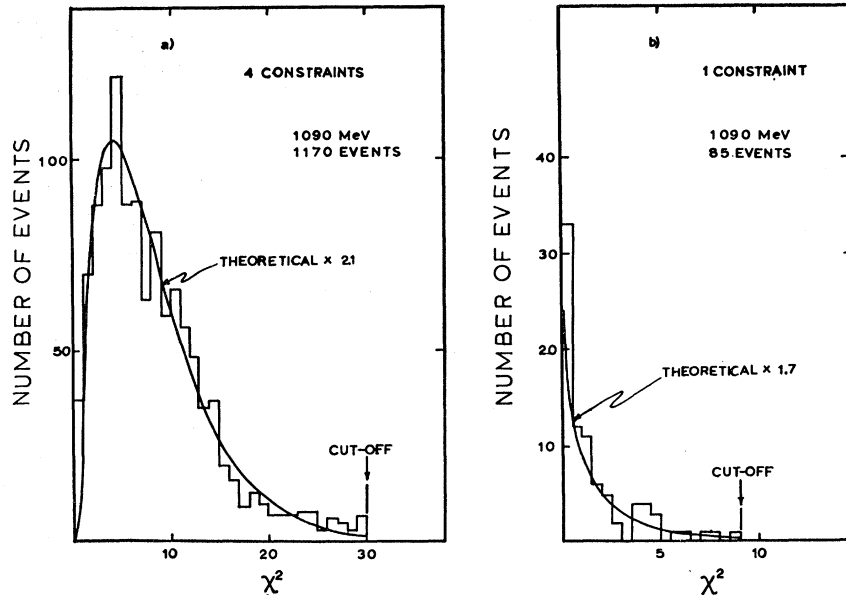
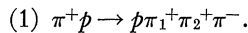
DISTRIBUTIONS OF χ^2


FIG. 1. χ^2 distribution for events at 1090 MeV. Theoretical χ^2 distributions fit the experimental one provided their horizontal scales are expanded by the factors indicated.

IV. DOUBLE PION PRODUCTION

In this section we discuss the production of two charged pions. The results are based on 1170 identified events at 1090 MeV, 870 events at 1260 MeV, and 65 events at 910 MeV of the type



Cross sections for production of two charged pions by reaction (1) are given in Table II.

Figure 2 shows the combined spectrum of the effective mass ($\pi_1^+ p$) and ($\pi_2^+ p$). It is apparent that the reaction is dominated by formation of the $N_{3/2, 3/2}^*$ isobar (mass 1238 MeV, and width $\Gamma \approx 90$ MeV). The influence of this isobar on other effective mass spectra may be very strong,¹⁵ and its effect must be carefully considered in searching for other resonances in these spectra.

A detailed attempt to fit the ($p\pi^+$) mass spectrum in reaction (1) in terms of the ($\pi^+ p$) scattering parameters¹⁶ has not been made. The kinematic effect of isobar

formation on the other spectra has been assessed, however, by multiplying the density of states in Lorentz-invariant phase space by the square of a transition amplitude describing the probability of isobar formation. Specifically, it is assumed that the transition amplitude is given by

$$A \approx \frac{(\Gamma/2)}{(M_1 - M_I) - i(\Gamma/2)} + \frac{(\Gamma/2)}{(M_2 - M_I) - i(\Gamma/2)},$$

where M_1 and M_2 are the effective masses $M(p, \pi_1^+)$ and $M(p, \pi_2^+)$, respectively, and M_I and Γ are the mass (1238 MeV) and the width (90 MeV) of the $(\frac{3}{2}, \frac{3}{2})$ resonant state. The amplitude A is symmetrized with respect to interchange of the two positive π mesons. These assumptions do not account for the observed long tail of the $M(p\pi^+)$ spectrum, as indicated by the dashed curve B on Fig. 2. They do, however, illustrate the kinematic effects of low ($p\pi^+$) effective masses and the symmetrization of A on the spectra of other effective mass combinations.

In Figs. 3 and 4 the effective mass spectra of the (π^+, π^-) system (two combinations per event) and the (π^+, π^+) system are shown. The prediction of Lorentz-invariant phase space does not fit the (π^+, π^-) mass spectrum and the agreement with the (π^+, π^+) spectrum is only fair. The kinematic effects of isobar formation and the symmetric role of the π^+ mesons are exhibited by the dashed curves B. One notes that the isobar concentrates the (π^+, π^+) masses at lower values and shifts the (π^+, π^-) masses towards high values.

In the calculation of curve B the angular distribution of the decay of the isobar in its own rest frame was as-

TABLE II. Cross sections for the reaction $\pi^+ p \rightarrow p \pi^+ \pi^+ \pi^-$.

Incident pion kinetic energies (MeV)	Energy in center of mass (MeV)	Cross section (mb)
910	1690	0.34 ± 0.06
1090	1790	1.04 ± 0.05
1260	1880	2.18 ± 0.14

¹⁵ R. M. Sternheimer and S. J. Lindenbaum, Phys. Rev. **123**, 333 (1961). This paper contains numerous references to the previous work of these authors on the Isobaric Nucleon Model.

¹⁶ M. Gell-Mann and K. M. Watson, Ann. Rev. Nucl. Sci. **4**, 219 (1954).

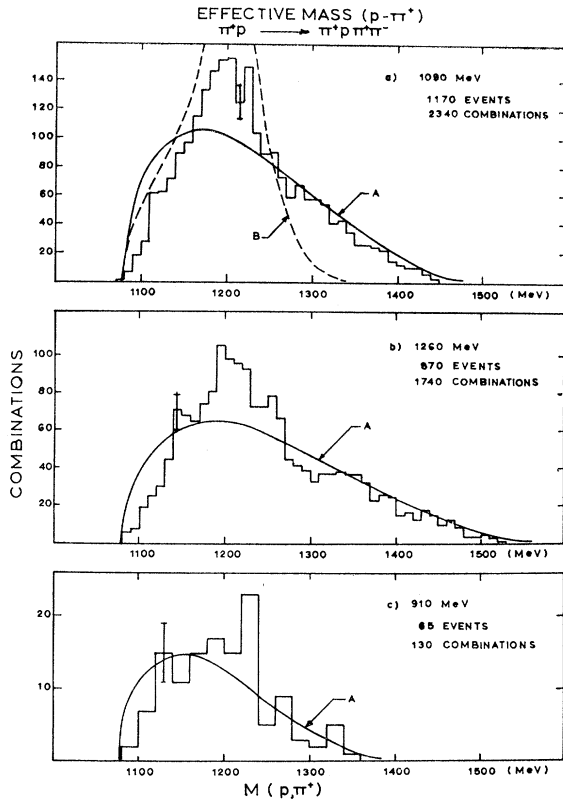


FIG. 2. Effective mass spectrum ($p\pi^+$) in the final state (p, π^+, π^+, π^-), each event contributing two combinations. Curve A is the prediction of Lorentz-invariant phase space, B is calculated using a Breit-Wigner transition amplitude, with $M_{\text{isobar}}=1220$ MeV and $\Gamma=90$ MeV and symmetrized with respect to interchange of the two π^+ mesons.

sumed isotropic. Nonisotropic isobar decay would leave the (π^+, p) mass spectrum unchanged but would introduce further distortions in the (π^+, π^-) spectrum.

Figure 5 shows the (p, π^+, π^+) effective mass spectrum. As expected, it disagrees with the predictions of phase space (curve A). Curve B shows, however, that the deviations may be entirely due to presence of the (π^+p) isobar. Thus the presence or absence of a $T=\frac{5}{2}$ resonant state in the (p, π^+, π^+) system cannot be determined.

The spectra of the effective masses (p, π^-) , (p, π^+, π^-) , and (π^+, π^+, π^-) have also been studied and show *no* enhancements that cannot be explained qualitatively as effects of the isobar.

The following conclusions are drawn from data presented in this section:

- (1) Formation of the $N^*_{3/2, 3/2}$ isobar state in the $(p\pi^+)$ dominates reaction (1).
- (2) A search for the ζ meson of mass ≈ 580 MeV in the (π^+, π^-) effective mass spectrum has not yielded any evidence for this particle. This observation supplements previous findings from the study of one-pion production in this experiment.

(3) No strong systematic enhancements are observed in the (π^+, π^+) spectrum in the mass region between 280 and 700 MeV.

(4) No evidence is found for the $T=\frac{5}{2}$ resonance, decaying into (p, π^+, π^+) , in the mass region from 1220 to 1700 MeV.

A study of the (π^+, p) spectrum in the final state of reaction (1) in terms of the (πp) scattering parameters, taking into account the Bose statistics for the two π^+ mesons, must be made, before further conclusions can be drawn from the data. An attempt of this type is suggested, for example, by the work of Dalitz and Miller¹⁷ on the subject of (Y^*) -production in K^-p reactions producing $(\Lambda^0, \pi^+, \pi^-)$ in the final state.

V. DECAY PROPERTIES OF THE η MESON

The primary analysis yielded 85 events at 1090 MeV, 94 events at 1260 MeV, and none at 910 MeV of the type

$$(2) \quad \pi^+p \rightarrow p\pi_1^+\pi_2^+\pi^-\pi^0.$$

(a) The Mass and Width of the η Meson

The effective mass spectrum for the combinations $M_1(\pi_1^+\pi^-\pi^0)$ and $M_2(\pi_2^+\pi^-\pi^0)$ in reaction (2) is strik-

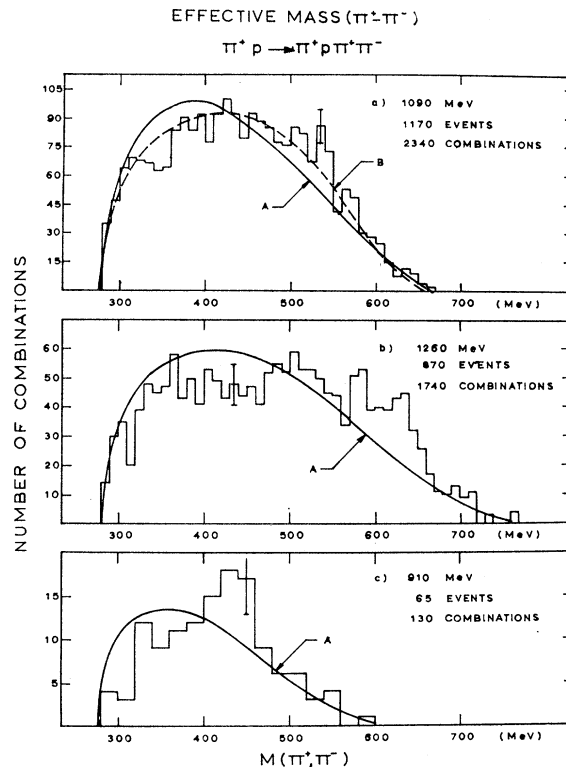


FIG. 3. Effective mass spectrum (π^+, π^-) in the final state (p, π^+, π^+, π^-), each event contributing two combinations. Curve A is the prediction of Lorentz-invariant phase space. Curve B illustrates the kinematic effects of an accumulation of events near the isobar mass (1220 MeV) in the $(p\pi^+)$ spectrum.

¹⁷ R. H. Dalitz and D. H. Miller, Phys. Rev. Letters 6, 562 (1961).

ingly inconsistent with uniform population of phase space. In fact 81 out of 85 events at 1090 MeV, and 77 out of 94 events at 1260 MeV have a combination M_1 or M_2 in the region $M=549\pm 20$ MeV (Fig. 6). Phase-space calculations on the 5-particle final state of reaction (2) predict only $\frac{1}{3}$ of the events (28 at 1090 MeV and 31 at 1260 MeV) in this mass region, when the mass combination closest to 549 MeV is selected. If one assumes events outside the mass region 549 ± 20 MeV to be distributed uniformly in phase space one obtains a background in the peak region of 2 events at 1090 MeV and 8 events at 1260 MeV. One concludes, therefore, that in 79 out of 85 cases at 1090 MeV and in 69 of 94 cases at 1260 MeV an η meson is produced.

The mass of the η meson is determined to be $M=549.0\pm 0.7$ MeV from the combined data at 1090 and 1260 MeV.

Measurement of the width of the η is limited by the experimental resolution. We have computed a resolution function by adding Gaussian error functions derived from errors computed by the χ ACK program, multiplied by $(1.7)^{1/2}$. The half-width of the resolution function for the 1090-MeV data is 7.1 MeV. The half-width of the experimental peak is 7.7 ± 0.7 MeV. As we have previously reported,⁹ these data are consistent with zero half-width (at half-maximum) of the η , and set an

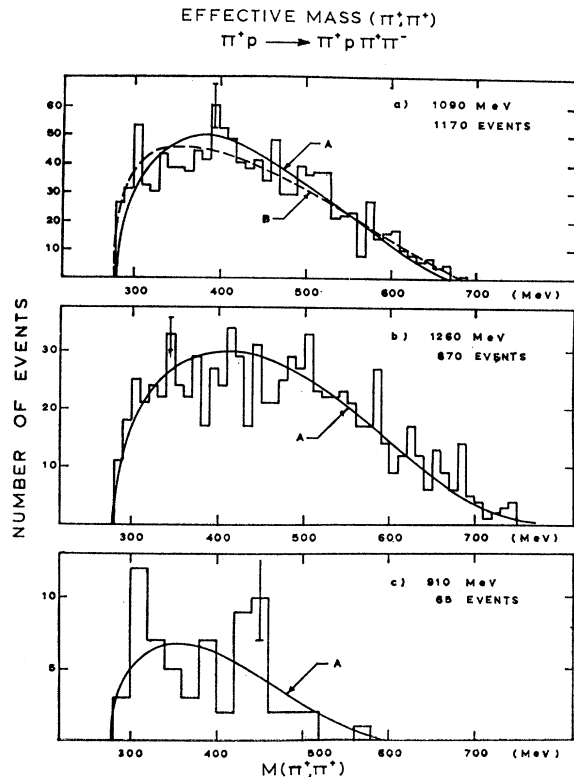


FIG. 4. Effective mass spectrum (π^+ , π^+) in the final state (p , π^+ , π^+ , π^-). Curves A and B are explained in the caption of Fig. 3.

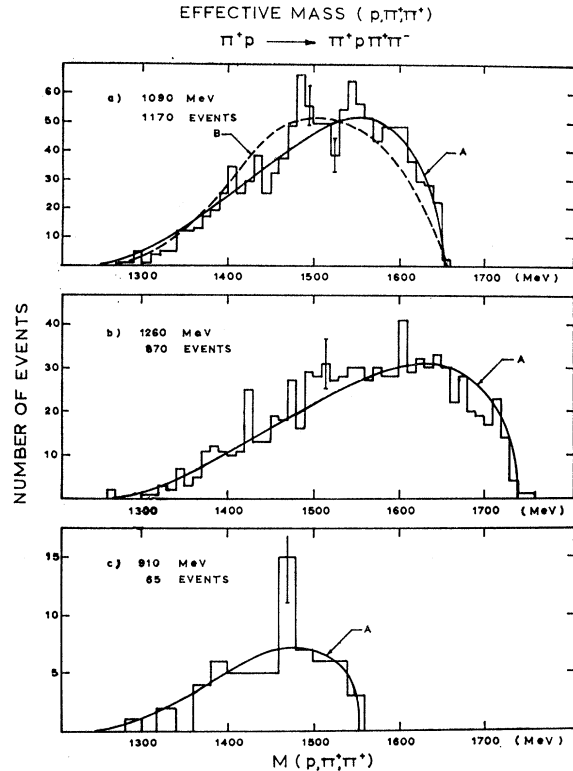


FIG. 5. Effective mass spectrum (p , π^+ , π^+) in the final state (p , π^+ , π^+ , π^-). Curves A and B are explained in the caption of Fig. 3.

upper limit of 5 MeV, consistent with results of other authors.^{5,18,19}

Figure 7 shows a scattergram of M_1 versus M_2 where the larger of the two masses has been labeled M_1 . About 17 of the 85 events have both M_1 and M_2 inside the region 549 ± 20 MeV. However, by choosing the mass closest to 549 MeV, we misidentify the η decay in only about 4 cases. If we identify the mass combination closest to and within 20 of 549 MeV, with the decay of the η meson, we obtain 81 events at 1090 MeV and 77 events at 1260 MeV and nonresonant backgrounds of 2% and 10%, respectively. Misidentification of the mass combination $M(\pi^+\pi^-\pi^0)$ resulting from the η decay contributes another 5% to the background. Reduced samples of 78 and 74 events, respectively, with M_1 or M_2 within 549 ± 15 MeV, will be used in discussions of the η decay Dalitz plot and the η production process.

¹⁸ See summary by G. Puppi, *Proceedings of the 1962 Annual International Conference on High Energy Physics at CERN*, edited by J. Prentki (CERN, Geneva, 1962), p. 713.

¹⁹ M. Meer, R. Strand, R. Kraemer, L. Madansky, M. Nussbaum *et al.*, *Proceedings of 1962 International Conference on High Energy Physics at CERN*, edited by J. Prentki (CERN, Geneva, 1962), p. 99; M. Foster, M. Good, R. Matsen, M. Peters, G. Tautfest, and R. Willmann, *ibid.*, p. 109; C. Alff, D. Colley, N. Gelfand, V. Nauenberg, D. Riller, J. Steinberger *et al.*, *ibid.*, p. 50, with D. Berley and J. Schulz, *Phys. Rev. Letters* **9**, 322, 325 (1962).

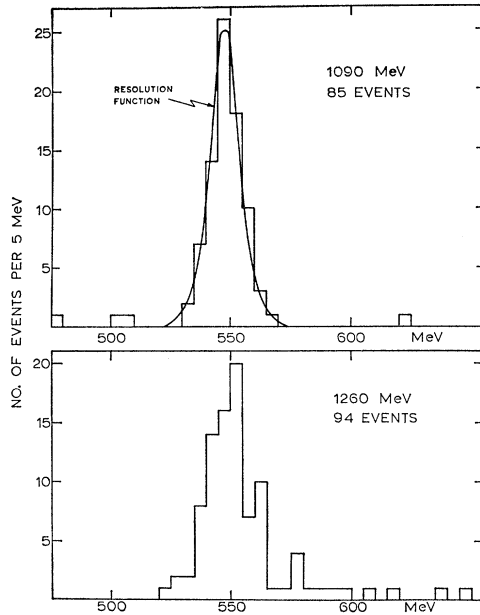


FIG. 6. Effective mass spectrum (π^+ , π^- , π^0) in the final state (p , π^+ , π^+ , π^- , π^0). Out of two possible combinations for each event the one closest to the value of 549 MeV is chosen.

(b) The Quantum Numbers of the η Meson

The isospin I , spin J , parity P , and G parity G of the η meson have been determined in several experiments. Since the original assignments of $I=0$ by Carmony *et al.*⁶ and $J^{PG}=0^{-+}$ by Bastien *et al.*,⁵ subsequent data^{18,19} have confirmed their conclusions. The present experiment, of which some results have been previously reported,^{8,9} provides further support.

In the following we perform a Dalitz analysis on the sample of η mesons obtained in this experiment. By comparing the experimental density of points on the Dalitz plot with theoretical predictions for all reasonably probable combinations of $I(J^{PG})$, one eliminates all combinations except for the G -violating decay of $0(0^{-+})$ or the allowed decay of $1(0^{-+})$.

That the η meson has isospin 0 rather than 1 has been shown in two independent ways:

1. The observation by Chretien *et al.*,²⁰ confirmed by Crawford *et al.*,²⁷ that the two-photon decay competes with the three-pion decay, shows that the three-pion decay violates G .

2. Charge independence arguments on the production reaction $\pi N \rightarrow p\eta$.⁶ Here we show that $I=1$ is also forbidden by charge independence in the reaction $\pi^+ p \rightarrow N\pi\eta$. To do this we assume $I=1$ and establish a lower limit on the amount of η^+ production in this reaction by applying charge independence. We then argue that η^+ should be detectable by the decay $\eta^+ \rightarrow (\pi^+\pi^+\pi^-)$. Our failure to observe η^+ , therefore,

²⁰ M. Chretien, F. Bulos, H. R. Crouch, Jr., R. E. Lanou, Jr., J. T. Massimo *et al.*, Phys. Rev. Letters **9**, 217 (1962).

contradicts the assumption that $I=1$. The detailed argument follows.

In Table I the simplest matrix elements are listed for η decay into three pions for all J^{PG} with $J \leq 1$ and $I \leq 1$. These predictions are compared to the Dalitz plot in Fig. 8.

The "Radial Density Plot" of Stevenson *et al.*³ is useful for comparison with the hypotheses of strong decay for $I=0$, $G=-1$, namely, $J^{PG}=0^{-+}$, 1^{+-} , 1^{-+} , all of whose simplest transitions into 3π 's predict symmetry of the Dalitz plot about each median of the Dalitz triangle. The density distribution as a function of distance from the center of the Dalitz plot is shown in Fig. 9(a). The experiment disagrees strongly with the prediction of $J^{PG}=1^{-+}$, shown as the solid curve. A 0^{-+} or a 1^{+-} matrix element would vanish at the center of the plot and rise sharply near the boundary, also in disagreement with the data.

Next we consider the three cases with $I=1$, $G=+1$. For $I=1$, $J^{PG}=0^{-+}$, the density should be independent of Y and should vanish on the Y axis, in disagreement with the data. For $I=1$, 1^{+-} the matrix element is identical to that for $I=0$, 1^{-+} , which was shown to be inconsistent with the data. The hypothesis $I=1$, 1^{++} would require a monotonically decreasing experimental distribution vanishing at maximum Y . The distribution does not decrease sufficiently strongly to agree with that prediction.

Finally, the three possibilities with $I=0$, $G=+1$ can be discussed together with the possibilities $I=1$, $G=-1$

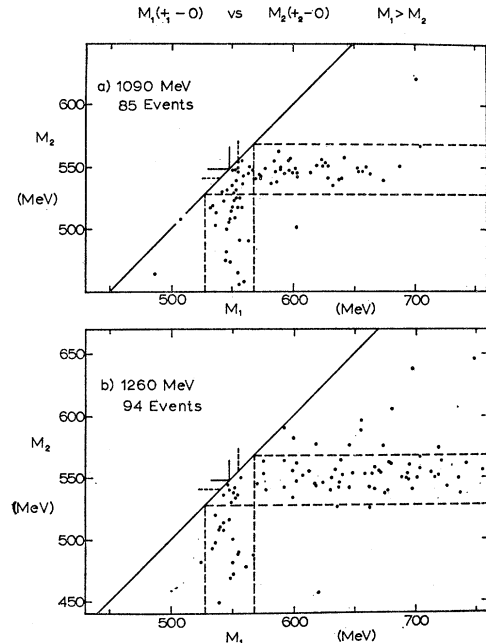


FIG. 7. Scattergram of $M_1(\pi^+, \pi^-, \pi^0)$ versus $M_2(\pi_2^+, \pi^-, \pi^0)$ in the final state (p , π_1^+ , π_2^+ , π^- , π^0) where the larger mass was labeled M_1 . The dashed lines define the region of masses $M=549 \pm 20$ MeV.

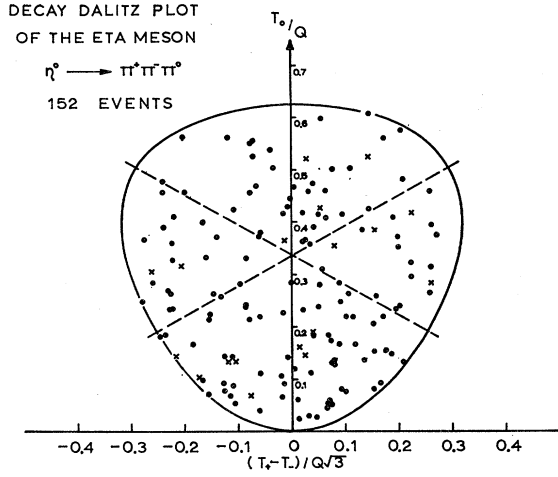


FIG. 8. Decay Dalitz plot of the η meson, 78 events at 1090 MeV and 74 events at 1260 MeV. Events with both mass combinations (π^+ , π^- , π^0) within 15 MeV of 549 MeV are indicated by (\times).

since both sets decay to an $I=1$ final state, so that the same theoretical predictions apply. For $I=0$, 1^- (and $I=1$, 1^-) the matrix element vanishes quadratically in X at the Y axis, and also on the boundary. For $I=0$, 1^{++} (and $I=1$, 1^{+-}) the experimental density of points would vanish at $Y=0$, increasing with increasing Y . None of these possibilities agree with the data; however, matrix elements for $I=0$, 0^+ or $I=1$, 0^- vanish nowhere and are consistent with the data, although the Dalitz plot deviates somewhat from their prediction of constant density. [See Fig. 9(b).] These conclusions agree with those previously reported^{5,9,18} and also with the observation of the $\gamma\gamma$ decay,²⁰ which eliminates $J=1$ and leaves only $J^P=0^-$, with $G=(-1)^I$. These two remaining possibilities can be distinguished by their I spin.

In their original assignment $I=0$, Carmony *et al.*⁶ applied charge independence to the reactions $\pi^+p \rightarrow$ Nucleon, η ; $\pi^+n \rightarrow$ Nucleon, η (from π^+-D reactions). We also find that $I=0$ from charge independence in our final state (π , nucleon, η), which requires a certain amount of η^+ production if $I=1$. We shall disprove now the possibility that $I=1$, using the data at 1090 MeV.

If $I=1$ this experiment should yield both η^0 and η^+ in the reaction channels

- (a) $\pi^+p \rightarrow \pi^+p\eta^0$,
- (b) $\pi^+p \rightarrow \pi^0p\eta^+$,
- (c) $\pi^+p \rightarrow \pi^+n\eta^+$.

The isospin part of the wave function in the final state, resulting from the initial state $T=\frac{3}{2}$, $T_z=\frac{3}{2}$, has the components

$$T_{3/2}^{3/2} \rightarrow a\left[\left(\frac{3}{5}\right)^{1/2}T_{3/2}^{3/2}\eta_1^0 - \left(\frac{2}{5}\right)^{1/2}T_{3/2}^{1/2}\eta_1^+\right] + bT_{1/2}^{1/2}\eta_1^+,$$

where η_1^0 , η_1^+ denote the isospin wave function of the η

with $I=1$ and $I_z=0, +1$ and the T 's are the isospin wave functions of the π -nucleon system. The ratio of η^+ to η^0 production is thus:

$$R = \frac{(\eta_1^+ \text{ production})}{(\eta_1^0 \text{ production})} = \frac{2}{3} + \frac{5}{3} \frac{|b|^2}{|a|^2},$$

which implies

$$R \geq 0.67.$$

The η production is detectable in this experiment by the decay modes $\eta^0 \rightarrow \pi^+\pi^-\pi^0$ and $\eta^+ \rightarrow \pi^+\pi^+\pi^-$. The η^0 decays into only neutrals at a relative rate^{5,18}

$$f_0 = \frac{(\eta^0 \rightarrow \text{all neutrals})}{(\eta^0 \rightarrow \pi^+\pi^-\pi^0)} = 3.0 \pm 0.5$$

and η^+ would go to (π^+ , neutrals) at some relative rate

$$f_1 = \frac{(\eta^+ \rightarrow \pi^+ \text{ neutrals})}{(\eta^+ \rightarrow \pi^+\pi^+\pi^-)}.$$

In terms of these ratios

$$R = \left(\frac{1+f_1}{1+f_0} \right) \left[\frac{(\eta^+ \rightarrow \pi^+\pi^+\pi^-)}{(\eta^0 \rightarrow \pi^+\pi^-\pi^0)} \right].$$

We do not observe any η^+ production in the modes

- (a) $\pi^+p \rightarrow \pi^0p(\pi^+\pi^+\pi^-)$,
- (b) $\pi^+p \rightarrow \pi^+n(\pi^+\pi^+\pi^-)$.

In reaction (a) only 4 out of 85 events are inconsistent with η^0 production ($\eta^0 \rightarrow \pi^+\pi^-\pi^0$), of which one event contains an effective mass of ($\pi^+\pi^+\pi^-$) within 20 MeV of the η mass. Three events of type (b) were observed, of which two are consistent with η^+ production. Ob-

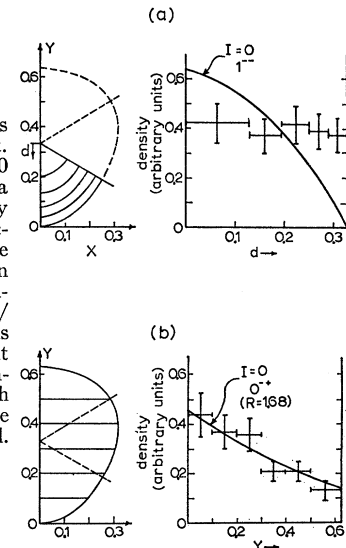


FIG. 9. (a) The analysis of the decay Dalitz plot. The prediction for $I=0$, $J^PG=1^-$ is shown as a solid curve. (b) Density on the Dalitz plot as a function of $Y=(T_0/Q)$. The solid curve is a prediction for $I=0$, 0^+_{-} and a branching ratio $R=(\eta \rightarrow 3\pi^0)/(\eta \rightarrow \pi^+\pi^-\pi^0)=1.68$. This curve takes into account the deviation from a constant matrix element which is expected if final-state interactions are considered.

TABLE III. Decay modes of a $0^- \eta$ meson.

Quantum numbers	Charge	I	Decay modes ^a	
			α	α^2
$I=0$ 0^{-+}	$Q=0$	$(4\pi^0)$	$(+-\gamma)$ $(+0\gamma)$	$(+-0), (000)$ $(\gamma\gamma)$ $(0\gamma\gamma)$
$I=1$ 0^{-}	$Q=0$	$(+-0), (000)$	$(+-\gamma)$ $(+0\gamma)$	$(+-0), (000)$ $(\gamma\gamma)$ $(0\gamma\gamma)$
	$Q=1$	$(++-), (+00)$	$(+0\gamma)$ $(++-\gamma), (+00\gamma)$	$(++-), (+00)$ $(+\gamma\gamma)$

^a $(+-0)$ means (π^+, π^-, π^0) .

servation of three or less η^+ events implies that the true number is less than 10 events with 99% confidence. Thus,

$$R < \left(\frac{1+f_1}{4} \right) \frac{10}{79}.$$

Anticipating the crucial result below that $f_1 < 1$ we find $R < 0.06$, which contradicts the requirement that $R \geq 0.67$ for $I=1$. This contradiction restricts the I spin of the η to $I=0$.

The crucial assertion is that f_1 is reasonably small. To be consistent with the requirement $R \geq 0.67$ for $I=1$, f_1 would have to be larger than 20. To see that this is improbable, we note that if $I=1$, J^{PG} can only be 0^- . In Table III the most probable decay modes for this case are summarized. The ratio $(\eta^+ \rightarrow \pi^+ \pi^0 \pi^0) / (\eta^+ \rightarrow \pi^+ \pi^+ \pi^-)$ can be shown to be $\frac{1}{4}$. Other decays into $(\pi^+, \text{neutrals})$ are of the order $\alpha = 1/137$ or α^2 . It appears very likely, therefore, that $f_1 < 1$, and almost certain that $f_1 < 20$.

(c) Final-State Interaction in the Three-Pion Decay

The experimental Dalitz plot does not agree with the prediction of a constant density for 0^{-+} , since the density decreases with increasing kinetic energy of the π^0 . This deviation from constant density [see Fig. 9(b)], may be explained by assuming final-state interactions. The problem has arisen before in connection with the τ decay of the K meson and the application to η decay has been discussed by Baqi Bég²¹ and by Wali.²² Both show that, assuming final-state interactions to be responsible for the observed distortions, the π^+ spectrum in the (π^+, π^0, π^0) decay of the K^+ should be similar to the π^0 spectrum of the (π^+, π^-, π^0) decay of the η^0 meson except for small effects due to the difference in mass of the K^+ and the η^0 . Assuming that the decay amplitude of the η can be expanded in powers of the pion kinetic energies, and retaining linear terms, the spectra can be described in terms of a single parameter. This parameter determines uniquely the decay ratio

$$r = (\eta \rightarrow \pi^0 \pi^0 \pi^0) / (\eta \rightarrow \pi^+ \pi^- \pi^0).$$

²¹ M. Baqi Bég, Phys. Rev. Letters **9**, 67 (1962).

²² K. C. Wali, Phys. Rev. Letters **9**, 120 (1962).

Figure 9(b) shows the square of the matrix element in arbitrary units as a function of the kinetic energy of the π^0 , and a theoretical expectation is drawn as a solid curve assuming $r=1.68$. The predicted spectrum is very sensitive to small changes in r ; for instance, $r=1.73$ would correspond to a uniform distribution. Within the limitations of the theoretical assumptions, therefore, the shape of the energy spectrum gives a very accurate indirect measurement of the ratio r .

The nature of the final-state interaction has been investigated in connection with the τ decay by various authors. Khuri and Treiman²³ and Sawyer and Wali²⁴ have assumed Mandelstam representations for the τ' decay amplitudes, and using S -wave $(\pi\pi)$ amplitudes they obtained solutions for the transition probabilities corresponding to repulsive S -wave $(\pi\pi)$ interactions. Since this result contradicted independent calculations for the $(\pi\pi)$ amplitudes in the $I=0, J=0$ state which were shown to be attractive, Baqi Bég and DeCelles²⁵ later suggested that the influence of P -wave interactions (ρ meson) should be appreciable.

An alternative approach has been given by Brown and Singer.²⁶ This argument assumes strong dipion-interaction enhanced in the region of effective $(\pi^+\pi^-)$ masses near 370 MeV with a width of ≈ 50 MeV. This interaction would produce enhancement for the π^0 spectrum of the η decay at kinetic energies between 10 and 45 MeV ($Y \approx 0.1$ to 0.3 on the Dalitz plot). Our data are statistically too weak to distinguish between these hypotheses, but they appear to favor the approach of Wali and Baqi Bég [see Fig. 9(b)]. However, Crawford *et al.*²⁷ have measured the $(3\pi^0)$ decay rate to be $r=0.83 \pm 0.32$, significantly lower than 1.68 required by Wali's theory, and their spectrum of π^0 kinetic energies favors the hypothesis of Brown and Singer.²⁶

(d) The (π^+, π^-, γ) Decay Mode

The observed relative decay rates of the η into $(\gamma\gamma)$, (3π) , and (π^+, π^-, γ) pose a difficulty for the assumption that the η has $J^{PG}=0^{-+}$ and $I=0$. The (π^+, π^-, γ) mode is of lower order in α than the 3π mode and also has more available phase space. The model of Brown and Singer attempts to explain the favored role of the (3π) decay compared to the $(\pi^+, \pi^-\gamma)$ decay. Also, the observed ratio $(\eta \rightarrow \pi^+ \pi^- \gamma) / (\eta \rightarrow \gamma\gamma)$ agrees with the " ρ dominant" model of Gell-Mann *et al.*,²⁸ which treats the eta as dissociating into two ρ mesons which couple to 2γ rays or to a γ ray and a $\pi^+ - \pi^-$ pair. This model

²³ N. N. Khuri and S. B. Treiman, Phys. Rev. **119**, 1115 (1960).

²⁴ R. F. Sawyer and K. C. Wali, Phys. Rev. **119**, 1429 (1960).

²⁵ M. Baqi Bég and P. C. DeCelles, Phys. Rev. Letters **8**, 46 (1962).

²⁶ L. M. Brown and P. Singer, Phys. Rev. Letters **8**, 460 (1962).

²⁷ F. S. Crawford, L. J. Lloyd, and E. C. Fowler, Phys. Rev. Letters **10**, 546 (1963). F. Crawford, Jr., R. Grossman, L. Lloyd, L. Price, and E. Fowler, *ibid.* **11**, 564 (1963).

²⁸ M. Gell-Mann, D. Sharp, and W. G. Wagner, Phys. Rev. Letters **8**, 261 (1962).

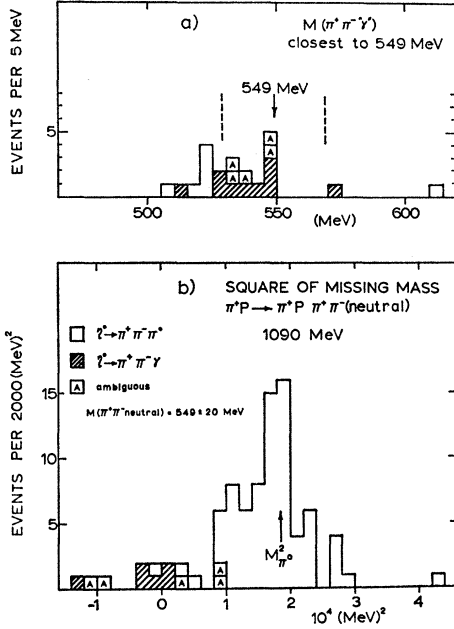


FIG. 10. The search for events consistent with $\eta \rightarrow \pi^+\pi^-\gamma$. The details of this search are explained in the text.

estimates that the $(\pi^+\pi^-\gamma)$ rate should be smaller than the $(\gamma\gamma)$ rate by a factor between $\frac{1}{4}$ and $\frac{1}{5}$. If the $(\gamma\gamma)$ decay rate is the same as the $\pi^+\pi^-\pi^0$, then the ratio $\Gamma(\pi^+\pi^-\gamma)/\Gamma(\pi^+\pi^-\pi^0)$ will also be between $\frac{1}{4}$ and $\frac{1}{5}$. The existence of the $\pi^+\pi^-\gamma$ decay has been established experimentally by Fowler *et al.*,³⁰ who find that $\Gamma(\pi^+\pi^-\gamma)/\Gamma(\pi^+\pi^-\pi^0) = 0.26 \pm 0.08$.

In principle the $(\pi^+\pi^-\gamma)$ decay mode should be detectable in this experiment by fitting events to the hypothesis $\pi^+\rho \rightarrow \rho\pi^+\pi^+\pi^-\gamma$, and studying the $(\pi^+\pi^-\gamma)$ mass spectrum. Practical difficulties arise since events which have no missing neutrals can always be fitted with a missing γ of sufficiently low momentum. The γ has zero mass and can account for any slight unbalance in the measured track momenta. If one attempts to fit a missing γ to events which have previously been successfully fitted as $\pi^+\rho \rightarrow \rho\pi^+\pi^+\pi^-$ one finds a spectrum of γ energies which has a maximum at zero and decreases rapidly with increasing energy. The occurrence of " γ " energy greater than 100 MeV is rare and each case has been traced to individual mismeasurements of short tracks. On the other hand, the spectrum of γ rays from $\pi^+\pi^-\gamma$ decay can be predicted roughly from the " ρ "-dominant model. The matrix element can be written²⁹

$$A \approx k^2 \frac{k_{\max} - k}{(1 + \beta k)^2},$$

where

$$k_{\max} = \left(\frac{M_\eta^2 - 4}{2M_\eta} \right) \approx \frac{3}{2}, \quad \beta = \left(\frac{2M_\eta}{M_\rho^2 - M_\eta^2} \right) \approx \frac{4}{7},$$

²⁹ R. Huff (private communication via E. C. Fowler).

and M_η , M_ρ , k are the η mass, ρ mass, and the γ -ray energy, respectively, in units of $m_\pi c^2$. Assuming for simplicity that the η 's decay at rest in the production center of mass, one finds that $\approx 70\%$ of all γ rays from the decay into (π^+, π^-, γ) have laboratory momenta larger than 100 MeV. We conclude that the events identified as $\pi^+\rho \rightarrow \rho\pi^+\pi^+\pi^-$ contain no η 's decaying as $\pi^+\pi^-\gamma$.

To isolate γ rays due to (π^+, π^-, γ) decay of the η , the sample originally identified as $\pi^+\pi^+\pi^-\pi^0$ (" π^0 events") and the sample of unidentified events (" γ question marks") were subjected to a computer search for a fit to the hypothesis

$$\pi^+\rho \rightarrow \rho\pi^+\pi^+\pi^-\gamma \quad (\gamma \text{ fit}).$$

For this fit it was required that $\chi^2 < 6.0$, missing mass < 100 MeV, $P_{\text{lab}}(\gamma) > 100$ MeV. A correction factor of 10/7 was applied to the final count, to account for events below the γ -momentum cutoff and we corrected for the missing mass cutoff with the factor 11/10. Only the 1090-MeV data were used. The results are summarized in Fig. 10. Figure 10(a) shows a spectrum of $(\pi^+\pi^-\gamma)$ effective mass for the combination closest to the η mass for each event successfully fitted as $\rho\pi^+\pi^+\pi^-\gamma$. The sample of π^0 events contains five possible $(\pi^+\pi^-\gamma)$ decays of the η [labeled "A" in Fig. 10(a)] and the sample of " γ question marks" contributes six possible events to give a total of at most 11. However, the events arising from previous π^0 fits form a cluster of $(\pi^+\pi^-\gamma)$ masses centered below 530 MeV, whereas they form an almost symmetric cluster within ± 15 MeV of 549 MeV if the π^0 fit is accepted as true. This suggests the correctness of their previous identification as π^0 . Also, the " γ question marks" (shaded events in Fig. 10) appear to contribute a background extending into the region of the eta mass. We thus estimate that the 11 possible $(\pi^+\pi^-\gamma)$ decays contain a background of about four events. The remaining 7 ± 4 $(\pi^+\pi^-\gamma)$ decays yield a branching ratio

$$\rho \rightarrow \eta \rightarrow (\pi^+\pi^-\gamma)/\eta \rightarrow (\pi^+\pi^-\pi^0) \approx 0.14 \pm 0.08.$$

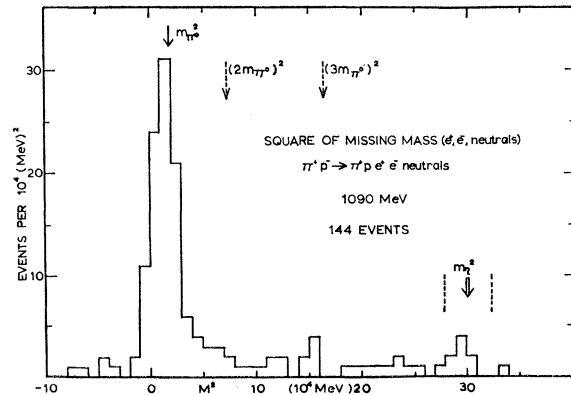


FIG. 11. Square of missing mass $M^2(e^+, e^-, \text{neutrals})$ in events of the type $\pi^+\rho \rightarrow \rho\pi^+e^+e^-$ (neutrals) calculated, using unfitted measurements of the protons and π^+ momenta.

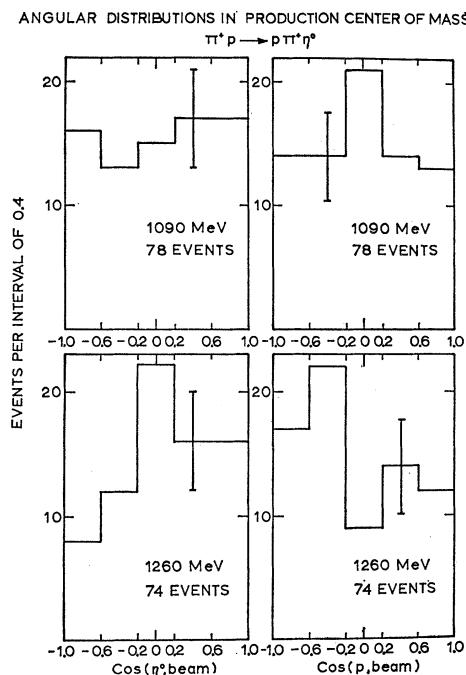


FIG. 12. Angular distributions of the η and the proton in the production center of mass in the reaction $\pi^+p \rightarrow \pi^+\pi^+\eta$.

This value of ρ is somewhat lower than the value 0.26 ± 0.08 reported by Fowler *et al.*³⁰ but is consistent within the uncertainties.

The spectrum of the square of the missing mass of 4-pronged events consistent with η formation after either a π^0 fit or a γ fit is shown in Fig. 10(b). Most of the weak cluster near zero missing mass are attributed to $\pi^+\pi^-\gamma$ decay.

(e) Other Decay Modes

The missing mass spectrum of $M^2[e^+, e^-, \text{neutral}(s)]$ from the Dalitz-pair-producing events $\pi^+p \rightarrow \pi^+pe^+e^-$ [neutral(s)] is shown in Fig. 11. Most of these events are Dalitz decays of π^0 from the final states $\pi^+p\pi^0$, $\pi^+p\pi^0\pi^0$, and $\pi^+p\pi^0\pi^0\pi^0$. The large peak at the π^0 mass contains the single π^0 production. There is also a small peak containing nine events in the region 549 ± 20 MeV. From phase-space extrapolation we expect only two or three events from $2\pi^0$ production and none from $3\pi^0$ production in this range. The average mass of the nine events is 544 ± 3 MeV. These nine events were fitted by the hypothesis

$$\pi^+p \rightarrow \pi^+p\eta^0[\eta^0 \rightarrow e^+e^- \text{neutral}(s)].$$

The missing mass of the neutral(s) exceeds 270 MeV in seven cases, and is definitely greater than 135 MeV in the other two. Thus none of the events can be the Dalitz decay $\eta^0 \rightarrow e^+e^-\gamma$. We assume that they are

³⁰ E. Fowler, F. Crawford, L. Lloyd, R. Grossman, and L. Price, Phys. Rev. Letters **10**, 110 (1963).

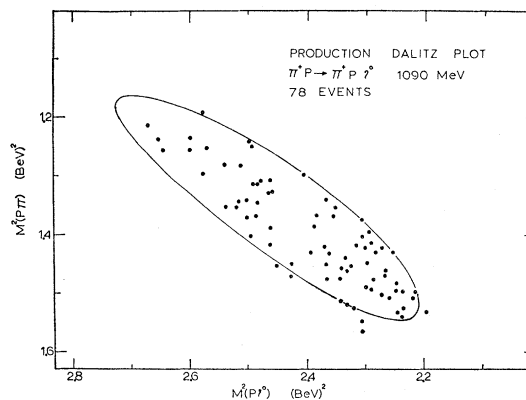


FIG. 13. Dalitz plot for η production at 1090 MeV. The concentration of events near maximum energy of the $(p\pi^+)$ system and minimum $(p\eta)$ energy is consistent with isobar formation in the $(p\pi^+)$ system or formation of the $T=1/2$ resonance of mass 1510 MeV in the $(p\eta)$ system.

instead $\eta^0 \rightarrow 3\pi^0 \rightarrow 2\pi^0 e^+ e^- \gamma$, with a background of three events. The remaining six events yield the branching ratio

$$R = (\eta \rightarrow 3\pi^0) / (\eta \rightarrow \pi^+\pi^-\pi^0) = 2.0 \pm 1.0.$$

Crawford *et al.*²⁷ have reported 0.83 ± 0.32 for this ratio.

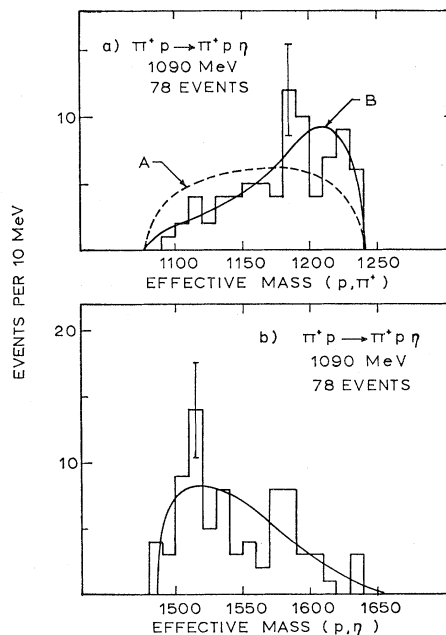


FIG. 14. Figure (a) shows that the distribution of effective masses (p, π^+) in the final state $p\pi^+\eta$ is inconsistent with the prediction of covariant phase space (dashed curve). The solid curve is calculated assuming 75% isobar formation and 25% nonresonant three-body background, added incoherently. Figure (b) shows the spectrum of the effective mass (p, η) in the same final state. The effect of isobar formation in the (p, π^+) system is reflected in this spectrum as shown by the solid curve ($M_{\text{isobar}} = 1220$ MeV, width $\Gamma = 90$ MeV, decay distribution of isobar $\approx 1 + 3 \cos^2\theta$).

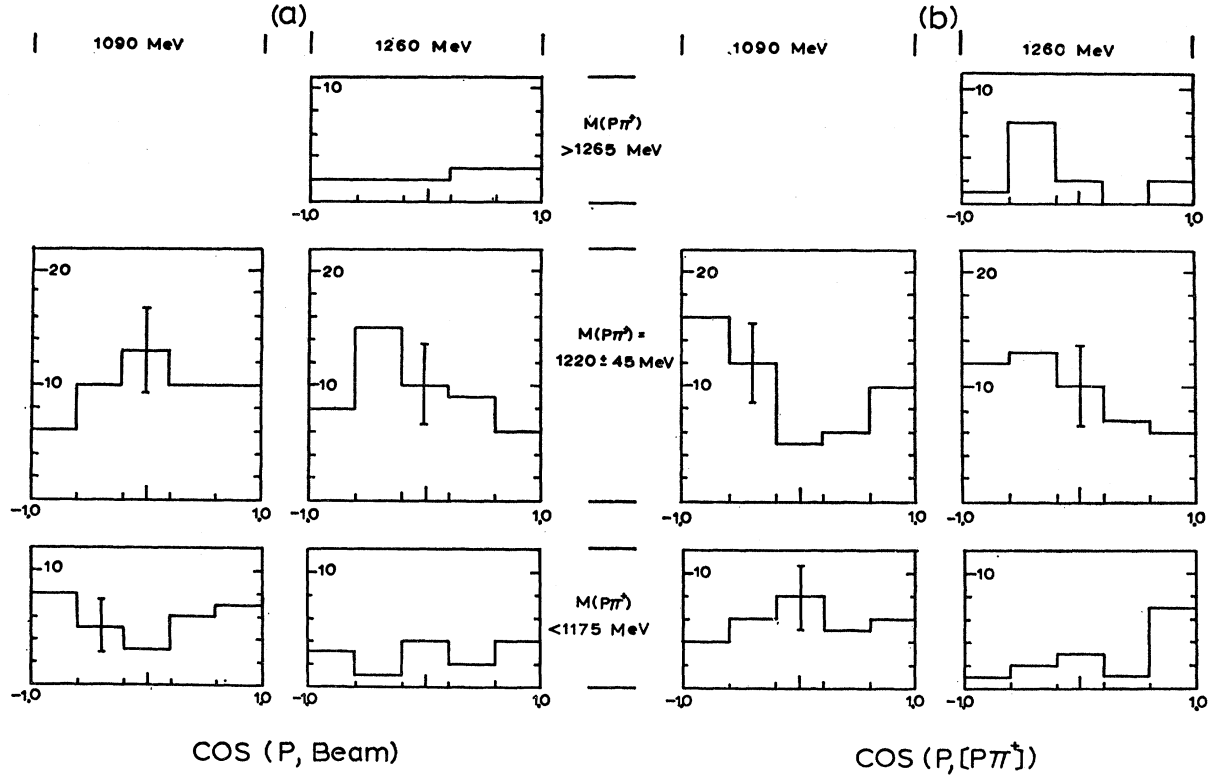


FIG. 15. Decay angular distributions of the $(p\pi^+)$ system at 1090 and 1260 MeV are shown separately for events having the effective mass (p, π^+) in the isobar region $[M(p\pi^+) = 1220 \pm 45 \text{ MeV}]$ and those with $M(p\pi^+)$ below or above this region: (a) Distribution in cosine θ , where θ is angle between beam direction and the decay proton. (b) Distribution in cosine θ' , where θ' is angle between decay proton and line of flight of isobar.

VI. THE η -PRODUCTION PROCESS

Between incident π^+ kinetic energies 910 and 1260 MeV, the η production cross section increases rapidly. Table IV exhibits the production cross sections for $\pi^+p \rightarrow \pi^+p\pi^+\pi^-\pi^0$ and for $\pi^+p \rightarrow \pi^+p\eta^0 \rightarrow \pi^+p\pi^+\pi^-\pi^0$. For the latter process, the angular distributions of the η meson and the proton in the reaction center of mass are shown in Fig. 12. These distributions do not exhibit the signature of peripheral interactions, namely, strong backward tendency of the proton. One notes in this connection that a single-particle exchange process, with an outgoing η at one vertex and the proton and π^+ at the other, is forbidden for exchange of a single π , ω , ρ , or η , since none of these could couple with a π^+ to produce a 0^{++} η meson with $I=0$.

The production Dalitz plot for the final state (π^+, p, η^0) is shown in Fig. 13. The concentration of events near minimum $(p-\eta^0)$ energy and maximum $(p\pi^+)$ energy suggests formation of the 1238-MeV π^+p isobar. This concentration could also be produced by final-state interaction of proton and eta, induced by the 1510-MeV isobar; this occurrence, however, should be inhibited by the angular momentum barrier and near-threshold energies. Figure 14(a) shows the agreement of the (π^+p) mass spectrum with a curve derived

by assuming the (π^+p) isobar is formed in 75% of the events. The agreement with 50% isobar formation is nearly as good, but there is definite disagreement with 0% formation (dashed curve). The $(p-\eta)$ mass spectrum shown in Fig. 14(b) agrees with the solid curve obtained by assuming that the 1238-MeV isobar is produced isotropically and decays with the distribution $1+3 \cos^2\theta$ along its line of flight. However, the maximum in the curve lies near 1510 MeV, so that the difficulty of distinguishing between formation of the 1239 and the 1510-MeV resonances is evident. In the following discussion we assume that the 1238-MeV isobar predominates.

The angular distributions of the "decay" proton in the center of mass of the secondary pion and proton are

TABLE IV. Production cross sections.

Energy (MeV)	Reaction $\pi^+p \rightarrow p\pi^+\pi^+\pi^-\pi^0$ (μb)	Reaction $\pi^+p \rightarrow \pi^+p\eta^0$ ($\pi^+\pi^-\pi^0$) decay only (μb)
910	<4 ^a	<4 ^a
1090	74 ± 8	69 ± 10
1260	220 ± 45	130 ± 45

^a No events seen.

presented in Fig. 15, with respect to both the direction of the incident π^+ [Fig. 15(a)] and the direction of motion of the secondary (π^+p) system [Fig. 15(b)]. These decay distributions can be predicted under certain simplifying assumptions. If the isobar is formed the small amount (a few MeV) of energy remaining in the center of mass suggests that only low angular momenta of the η are produced, of which the S state may be most prominent. The isobar in the final state, therefore, should have a decay distribution of $|Y_{3/2}^{1/2}|^2 \rightarrow 1 + 3 \cos^2\theta$ with respect to the direction of the incident π^+ . The experimental distributions for the two energies 1090 and 1260 MeV, shown in Fig. 15(a), are inconsistent with this prediction for events in the isobar peak [$M(p\pi^+) = 1220 \pm 45$ MeV]. The assumption of pure S -wave production in conjunction with pure isobar is therefore incorrect. High angular momenta of the η or final-state interaction can invalidate this assumption.

The distribution of the polar angle θ' of the proton from the isobar decay with respect to its line of flight [Fig. 15(b)] also contains information on the final-state

angular momenta. The distribution for 1090 MeV in Fig. 15(b) shows forward-backward peaking for events in the isobar mass region, consistent with isobar formation together with P - or D -wave emission of the η . At 1260 MeV some odd power of $\cos\theta'$ is present whose coefficient changes sign as the effective mass of the $(p\pi^+)$ combination passes through the isobar region. This may be caused by background interference with a resonating P wave (isobar) in the decay of the $(p\pi^+)$ system.

ACKNOWLEDGMENTS

It is a pleasure to acknowledge the cooperation of the Bubble Chamber Group at Brookhaven, under the direction of Dr. Ralph Shutt, and of the Cosmotron Department and the A.G.S. Department. J. R. Sanford, H. W. Courant, and E. C. Fowler participated in this experiment in its early stages. The continued financial assistance of the U. S. Atomic Energy Commission and the National Science Foundation is gratefully acknowledged.